

First-order Fermi acceleration at pulsar wind termination shock

Simone Giacchè¹, John Kirk¹, Takanobu Amano²

¹Max-Planck-Institut für Kernphysik, Heidelberg, Germany

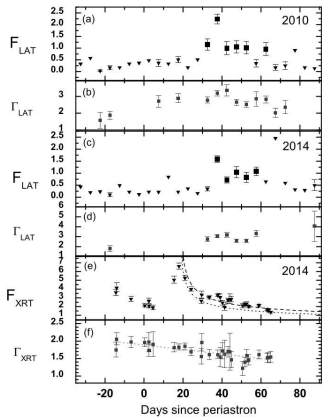
²Department of Earth & Planetary Science, University of Tokyo, Japan

28th Texas Symposium on Relativistic Astrophysics

Genève 14 December 2015

Motivation

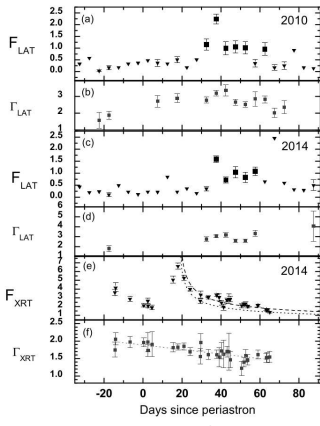
PSR B1259-63



Tam *et al.* 2015

Motivation

PSR B1259-63



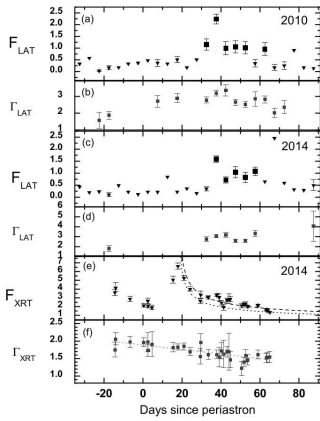
Tam *et al.* 2015

- superluminal waves for $\omega > \omega_{p0}$
- electromagnetically modified shock
- relevant in the context of γ -ray binaries

Amano & Kirk 2013

Motivation

PSR B1259-63



Tam *et al.* 2015

- superluminal waves for $\omega > \omega_{p0}$
- electromagnetically modified shock
- relevant in the context of γ -ray binaries

Amano & Kirk 2013

Goal: investigate the effects of the electromagnetically modified shock on particle acceleration

Outline

1 Simulation of the pulsar wind

- investigation of different ω , σ and Γ
- precursor steady states

2 Test particle approach

- reflection probability
- energy spectrum

3 Simulation of Fermi-like process

- pure scattering + normal deflection upstream, scattering downstream
- pulsar wind upstream, scattering downstream
- different regimes for λ' , r'_g , L'_{scatt}

Simulation of the pulsar wind

Set-up

- two relativistic fluids (e^- , e^+)
- 1D simulation
- ultra-relativistic shock Γ_s
- magnetised flow

$$\sigma = \frac{\text{Poynting flux}}{\text{particle kinetic energy density}}$$

The wind

- fully transverse, circularly polarised magnetic shear wave
- null phase-averaged magnetic field
- $\omega \propto \omega_{p0}$ with $\omega_{p0} = \sqrt{\frac{8\pi ne^2}{m}}$
(upstream proper plasma frequency)

Simulation of the pulsar wind

Set-up

- two relativistic fluids (e^- , e^+)
- 1D simulation
- ultra-relativistic shock Γ_s
- magnetised flow
$$\sigma = \frac{\text{Poynting flux}}{\text{particle kinetic energy density}}$$

$$\text{runs } \omega = 1.2\omega_{p0}$$

Γ	σ
10	10
	25
	100
40	10
	50
50	25
	100
70	10
	50
	100
100	25
	50
	100

The wind

- fully transverse, circularly polarised magnetic shear wave
- null phase-averaged magnetic field
- $\omega \propto \omega_{p0}$ with $\omega_{p0} = \sqrt{\frac{8\pi ne^2}{m}}$
(upstream proper plasma frequency)

Simulation of the pulsar wind

Set-up

- two relativistic fluids (e^- , e^+)
- 1D simulation
- ultra-relativistic shock Γ_s
- magnetised flow
$$\sigma = \frac{\text{Poynting flux}}{\text{particle kinetic energy density}}$$

$$\text{runs } \omega = 1.2\omega_{p0}$$

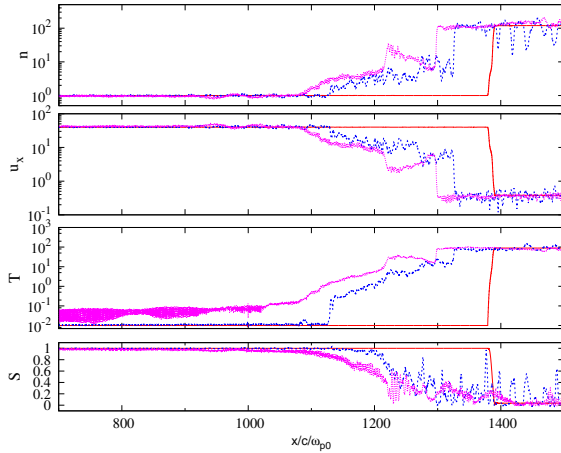
Γ	σ	
10	10	
	25	
	100	
40	10	RUN A
	50	
50	25	
	100	
70	10	
	50	
	100	
100	25	RUN B
	50	
	100	

The wind

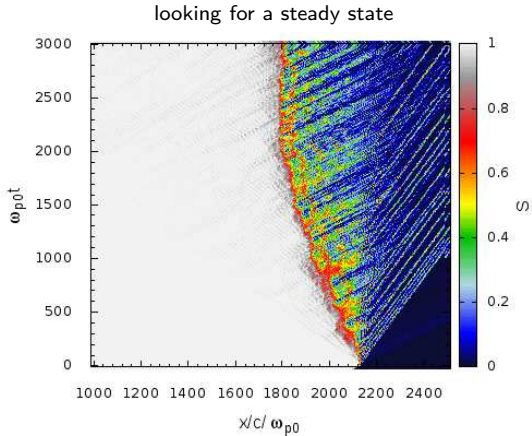
- fully transverse, circularly polarised magnetic shear wave
- null phase-averaged magnetic field
- $\omega \propto \omega_{p0}$ with $\omega_{p0} = \sqrt{\frac{8\pi ne^2}{m}}$
(upstream proper plasma frequency)

Run A: $\Gamma = 40$, $\sigma = 10$

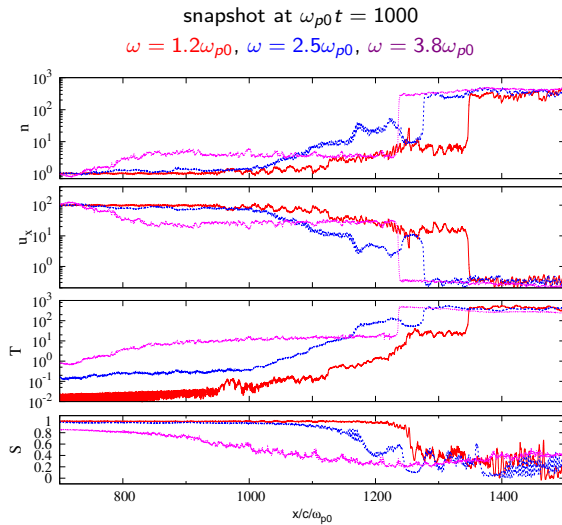
snapshot at $\omega_{p0}t = 1000$
 $\omega = 0.4\omega_{p0}$, $\omega = 1.2\omega_{p0}$, $\omega = 2.5\omega_{p0}$



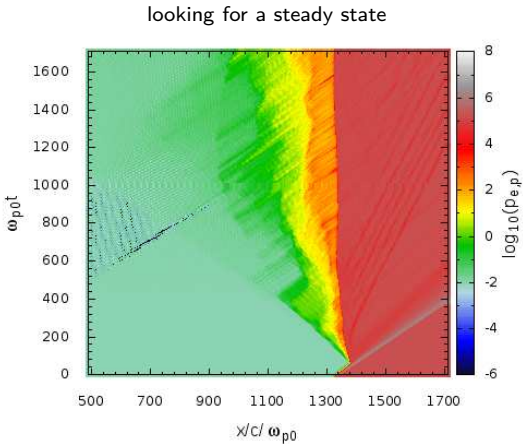
Run A: $\Gamma = 40$, $\sigma = 10$, $\omega = 1.2\omega_{p0}$



Run B: $\Gamma = 100$, $\sigma = 25$



Run B: $\Gamma = 100$, $\sigma = 25$, $\omega = 1.2\omega_{p0}$



$\omega_{p0} t [0 : 1700]$, $x/c/\omega_{p0} [0 : 2000]$

$$x_{sh}/c/\omega_{p0} = 1335$$

Numerical integration of particle trajectories

$$\frac{d\vec{x}}{dt} = \vec{\beta}$$

$$\frac{d\vec{n}}{dt} = \frac{q}{m\gamma\beta} [\vec{E}_\perp + \vec{\beta} \times \vec{B}]$$

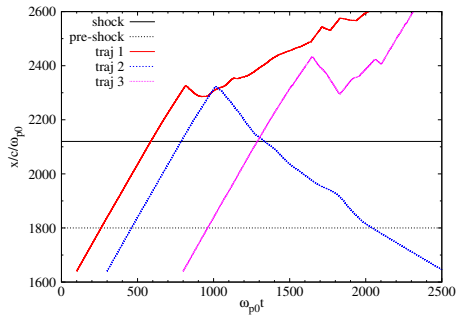
$$\frac{d\gamma}{dt} = \frac{q}{mc} \beta \vec{n} \cdot \vec{E}$$

using 4th order Runge-Kutta method in the test particle limit

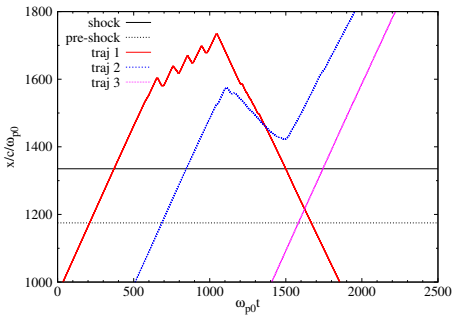
Trajectories started off far upstream of the shock with isotropic distribution in the upstream fluid frame.

Typical trajectories

RUN A



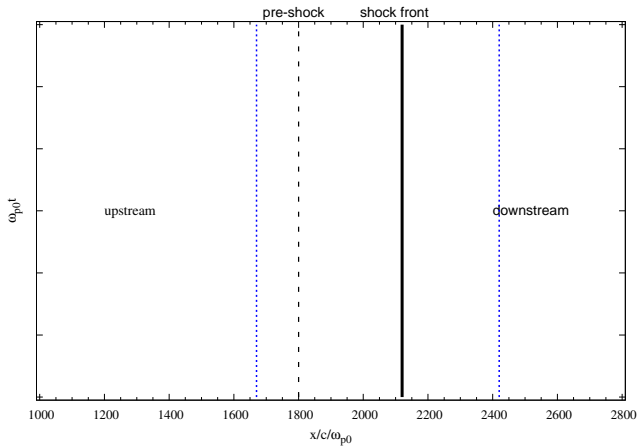
RUN B



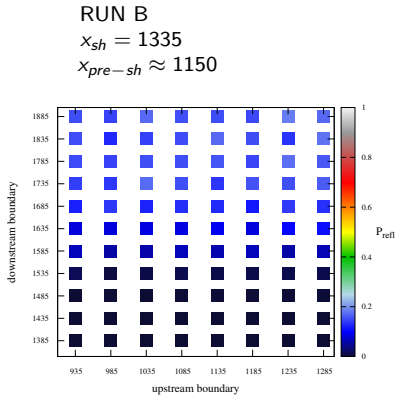
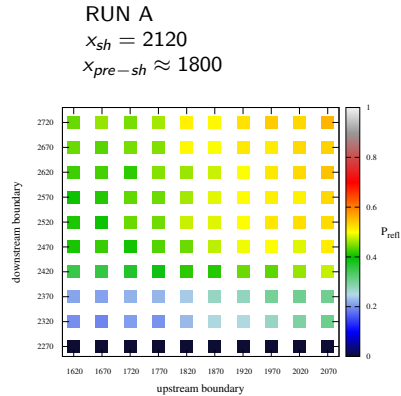
Particles are followed until they reach either one of the two spatial boundaries of the simulation box.

Injection/reflection probability

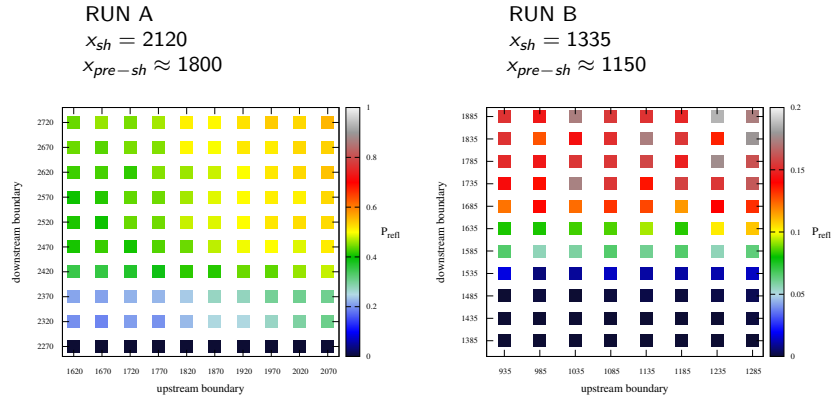
we set upstream and downstream absorbing boundaries to record particles



Injection/reflection probability



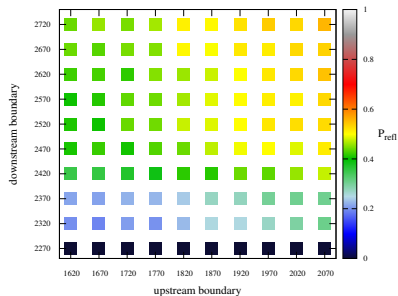
Injection/reflection probability



Injection/reflection probability

RUN A

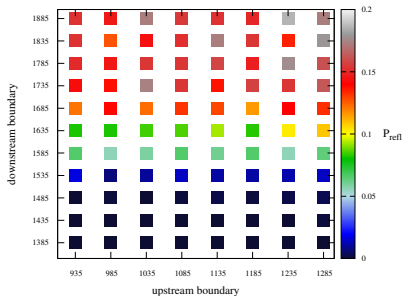
$$x_{sh} = 2120$$
$$x_{pre-sh} \approx 1800$$



$$P_{refl} \sim 0.44$$

RUN B

$$x_{sh} = 1335$$
$$x_{pre-sh} \approx 1150$$



$$P_{refl} \sim 0.15$$

$P_{refl} \sim 0.12$ for ultrarelativistic, perpendicular shocks (Achterberg *et al.* 2001)

Energy spectrum

RUN A

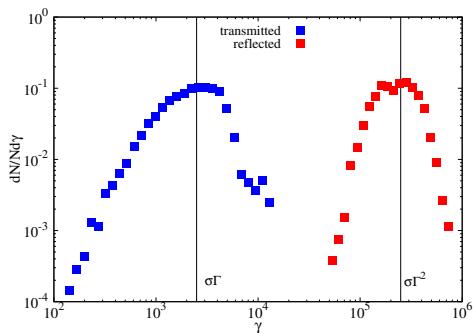
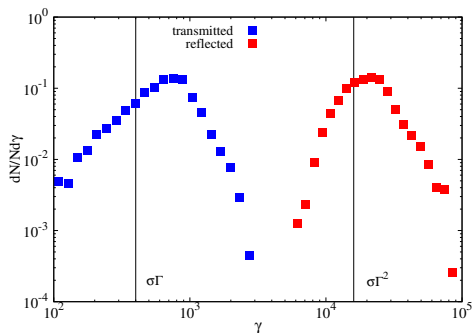
upstream boundary $x_{up} = 1670$

downstream boundary $x_{down} = 2720$

RUN B

upstream boundary $x_{up} = 985$

downstream boundary $x_{down} = 1885$

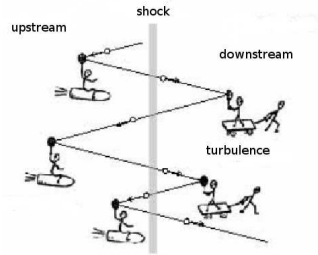


$$\gamma'_{inj} \approx \sigma\Gamma^2 \text{ in the upstream fluid frame}$$

First-order Fermi acceleration

Monte Carlo technique

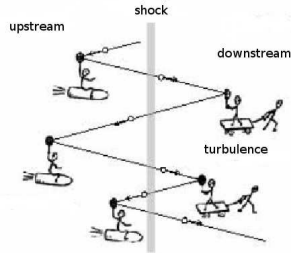
- elastic scattering in the local fluid frame
- isotropic diffusion
- $f(p, \mu) = p^{-s} g(\mu)$



First-order Fermi acceleration

Monte Carlo technique

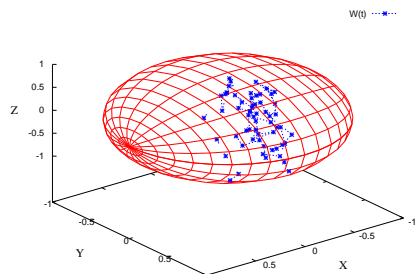
- elastic scattering in the local fluid frame
- isotropic diffusion
- $f(p, \mu) = p^{-s} g(\mu)$



$$d\vec{n} = \vec{a}(x, t) * dt + \vec{b}(x, t) * dW(t)$$

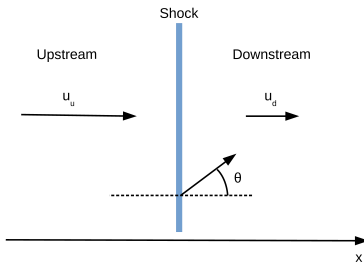
e.g. Itoh 1944, Achterberg & Krülls 1992

small angle scattering $\delta\psi \ll 1/\Gamma \Rightarrow D_\theta$



Injection conditions in the upstream frame

- location: at the shock front
- direction: $\mu'_{inj} = -1$
- energy: $\gamma'_{inj} = \sigma \Gamma^2$



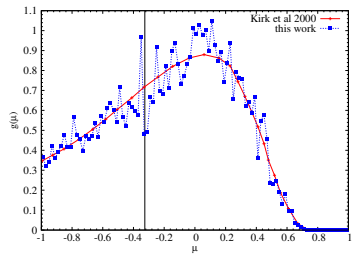
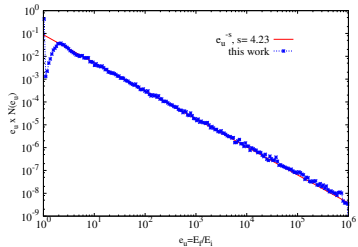
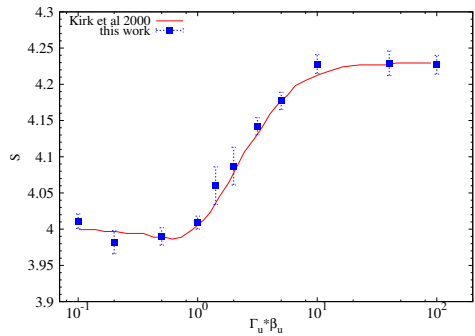
$$\mu = \cos \theta$$

The trajectory integration is performed in the local fluid frame.

Deflection: case of pure scattering

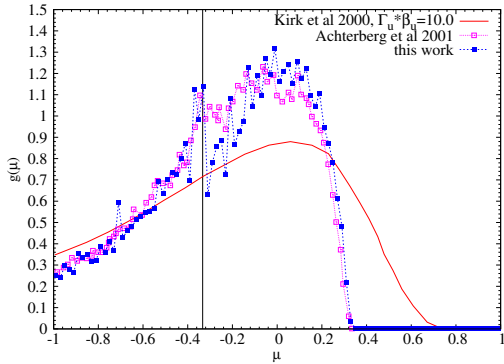
$$\Gamma_u * \beta_u = 10.0$$

Comparison with the results of the eigenfunction method (Kirk et al. 2000) for different values of $\Gamma_u * \beta_u$.



Deflection: regular deflection upstream, scattering downstream

$$\Gamma_u * \beta_u = 100.0$$



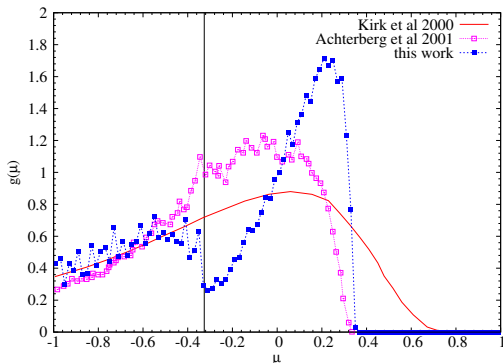
	Achterberg et al. 2001	this work
Γ_s	s	s
10	4.28 ± 0.01	4.28 ± 0.01
100	4.30 ± 0.01	4.30 ± 0.01

Deflection: pulsar wind upstream, regime I

Characteristic length-scales upstream

- $\lambda' = \frac{2\pi\beta_s\Gamma_s}{\omega}$ ($\Gamma_u * \beta_u = 10.0$)
- $L'_{scatt} = ct'_{scatt} = c/2D_\theta$ ($\Delta\theta \sim 1/\Gamma$)
- $r'_g = \gamma'/eB'$

$$L'_{scatt} \sim \lambda' \gg r'_{g,\max} \implies s = 4.28 \pm 0.01$$

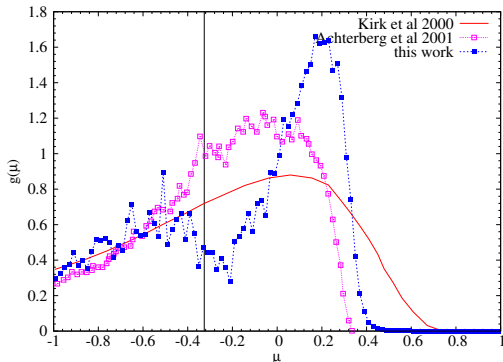


Deflection: pulsar wind upstream, regime II

Characteristic length-scales upstream

- $\lambda' = \frac{2\pi\beta_s\Gamma_s}{\omega}$ ($\Gamma_u * \beta_u = 10.0$)
- $L'_{scatt} = ct'_{scatt} = c/2D_\theta$ ($\Delta\theta \sim 1/\Gamma$)
- $r'_g = \gamma'/eB'$

$$L'_{scatt} \gg r'_{g,\max} \gg \lambda' \gg r'_{g,\min} \implies s = 4.26 \pm 0.01$$

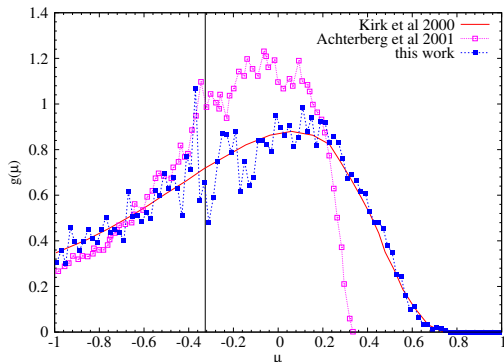


Deflection: pulsar wind upstream, regime III

Characteristic length-scales upstream

- $\lambda' = \frac{2\pi\beta_s\Gamma_s}{\omega}$ ($\Gamma_u * \beta_u = 10.0$)
- $L'_{scatt} = ct'_{scatt} = c/2D_\theta$ ($\Delta\theta \sim 1/\Gamma$)
- $r'_g = \gamma'/eB'$

$$r'_{g,\max} \gg L'_{scatt} > r'_{g,\min} \sim \lambda' \implies s = 4.23 \pm 0.01$$



Realistic pulsar wind

$$\sigma = \frac{B^2}{4\pi \sum_s \Gamma_s w_s u_{s,x}} \quad B'_0 = \sqrt{8\pi\sigma}$$

the specific enthalpy in the cold wind is

$$w_s = n_s m_s c^2$$

$$\lambda' = \frac{2\pi\beta_s\Gamma_s}{\omega} \quad r'_g = \gamma/\sqrt{\sigma}$$

$$\omega_{p0} = m = c = 1, e = 1/\sqrt{8\pi}$$

we showed that $\gamma'_{inj} \approx \sigma\Gamma_s^2$ for both RUN A and RUN B

$$\frac{\lambda'}{r'_g} = \frac{2\pi\beta_s}{\omega\sqrt{\sigma}\Gamma_s} \ll 1 \implies s = 4.23$$

Summary

① Simulation of the pulsar wind

- investigation of parameter space (Γ, σ, ω)
- precursor steady state for $\Gamma = 40$, $\sigma = 10$ and $\Gamma = 100$, $\sigma = 25$ for $\omega = 1.2\omega_{p0}$

② Test particle approach

- RUN A $P_{inj} \sim 0.44$, RUN B $P_{inj} \sim 0.15$
- injection energy $\gamma'_{inj} \approx \sigma\Gamma^2$

③ Simulation of Fermi-like process

- results of our code in perfect agreement with semi-analytical (Kirk *et al.* 2000) and numerical (Achterberg *et al.* 2001) works
- study of the effects of the pulsar wind (magnetic shear) in different regimes
- for realistic pulsar wind $\lambda'/r'_g \ll 1$ and $s = 4.23$

Summary

① Simulation of the pulsar wind

- investigation of parameter space (Γ, σ, ω)
- precursor steady state for $\Gamma = 40$, $\sigma = 10$ and $\Gamma = 100$, $\sigma = 25$ for $\omega = 1.2\omega_{p0}$

② Test particle approach

- RUN A $P_{inj} \sim 0.44$, RUN B $P_{inj} \sim 0.15$
- injection energy $\gamma'_{inj} \approx \sigma\Gamma^2$

③ Simulation of Fermi-like process

- results of our code in perfect agreement with semi-analytical (Kirk *et al.* 2000) and numerical (Achterberg *et al.* 2001) works
- study of the effects of the pulsar wind (magnetic shear) in different regimes
- for realistic pulsar wind $\lambda'/r'_g \ll 1$ and $s = 4.23$

THANK YOU FOR YOUR ATTENTION

BACK UP SLIDES

Magnetic shear wave

Lab. frame (Shock frame)

$$B_x = 0$$

$$B_y = B_0 \cos(kx - \omega t)$$

$$B_z = -B_0 \sin(kx - \omega t)$$

$$E_x = 0$$

$$E_y = \beta B_z$$

$$E_z = -\beta B_y$$

$$k = \omega/\beta$$

$$\omega = 1.2\omega_{p0}$$

$$\lambda = 2\pi\beta/\omega$$

Upstream fluid frame

$$B_x' = 0$$

$$B_y' = B_y/\Gamma$$

$$B_z' = B_z/\Gamma$$

$$E_x' = 0$$

$$E_y' = 0$$

$$E_z' = 0$$

$$k' = k/\Gamma$$

$$\omega' = 0$$

$$\lambda' = 2\pi\beta\Gamma/\omega$$

$$\beta = \sqrt{1 - 1/\Gamma^2}, \quad \omega_{p0} = \sqrt{\frac{8\pi ne^2}{m}}, \quad \bar{k} = (k, 0, 0)$$

Flux at the upstream boundary

RUN A

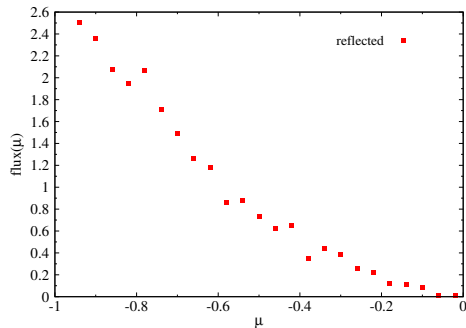
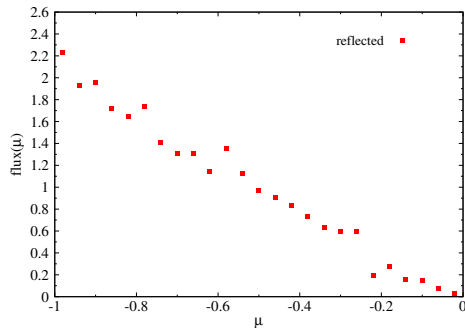
upstream boundary $x_{up} = 1670$

downstream boundary $x_{down} = 2720$

RUN B

upstream boundary $x_{up} = 985$

downstream boundary $x_{down} = 1885$



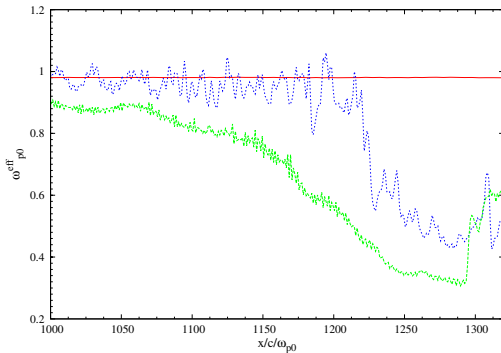
$$\mu = \cos \theta$$

$\mu'_{inj} \approx -1$ in the upstream fluid frame

Run A: $\Gamma = 40$, $\sigma = 10$

enlarged view of the precursor, snapshot at $\omega_{p0}t = 1000$

$$\omega = 0.4\omega_{p0}, \omega = 1.2\omega_{p0}, \omega = 2.5\omega_{p0}$$

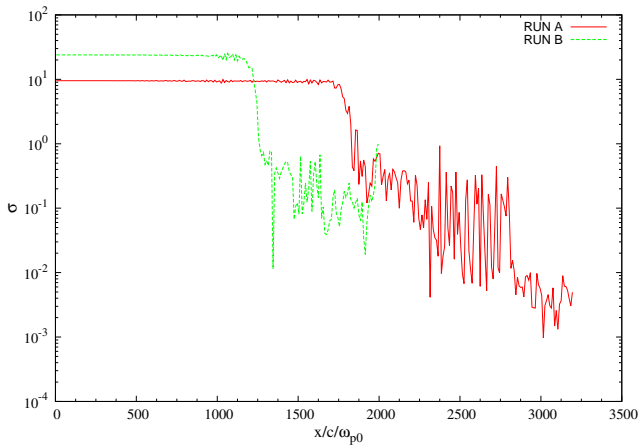


$$\omega_{p0}^{eff} = \sqrt{\frac{8\pi ne^2}{mh}}$$

$$h = 1 + \frac{\gamma_h}{\gamma_h - 1} \frac{T}{mc^2}, \quad \gamma_h = 4/3 \text{ ratio of specific heat}$$

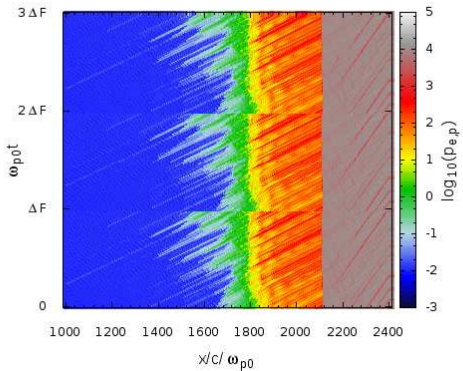
RUN A and B, σ comparison

RUN A: $\Gamma = 40, \sigma = 10$
RUN B: $\Gamma = 100, \sigma = 25$



Time domain periodic boundaries

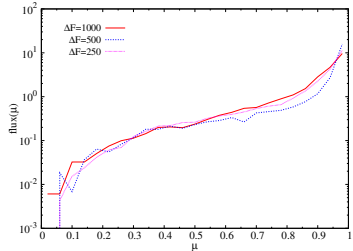
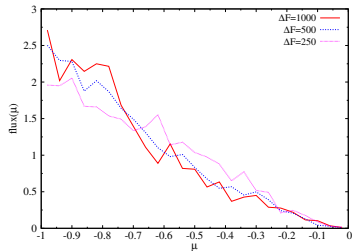
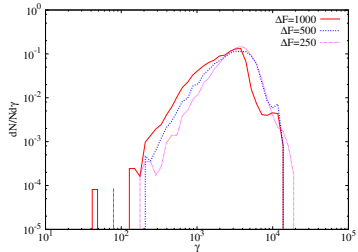
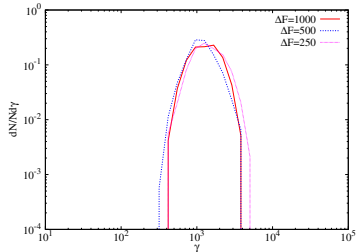
folding ensemble of snapshots ΔF



We tested energy spectrum and angular distribution at both ends of the simulation box for different foldings, but same overall integration time.

Spectrum and angular distribution with periodic boundaries

overall integration time ~ 8000 for different values of ΔF



Acceleration region limited in size

dependence of the spectral index s on the size of the acceleration region
compared to L_{scatt}

